J Appl Electrochem (2008) 38:167–173
DOI 10.1007/s10800-007-9420-3

ORIGINAL PAPER

Galvanostatic Pb(II) removal from a simulated wastewater by using a stainless-steel wool cathode in a flow-through cell: a factorial-design study

Lucio C. Almeida · Luiz H. S. Gasparotto · Nerilso Bocchi · Romeu C. Rocha-Filho · Sonia R. Biaggio

Received: 17 May 2007 / Revised: 23 August 2007 / Accepted: 10 September 2007 / Published online: 2 October 2007

Abstract The response surface methodology was used to find the optimal condition for electrolytic Pb(II) removal by using, as the experimental design, a central composite rotatable design for two variables (current and flow rate) at five levels. The surfaces generated with the second-order-equation fitted data showed the positive influence of increasing the current variable on the removal efficiency, leading to 93% removal after 30-min electrolysis. However, high current values lowered the current efficiency due to parasitic reactions. On the other hand, the flow rate variable did not substantially affect either the removal or the current efficiency. Electrolysis carried out at the optimised condition (250 L h^{-1} and –0.25 A), after 90-min electrolysis, lowered the Pb(II) concentration from 50 ppm to 0.5 ppm, corresponding to 99% removal.

Keywords Factorial design · Response surface methodology · Electrolytic wastewater treatment · Stainless-steel wool · Three-dimensional cathode · Flow-through cell

1 Introduction

The treatment of industrial effluents containing toxic metallic ions like Pb(II), Cd(II) and Cr(VI) is required in order to decrease their concentrations to acceptable levels before discharge [1–6]. The treatment of industrial wastewaters is usually carried out by adjusting the solution pH or adding a suitable counter-ion to form precipitates. Despite the fact that this method is efficient in removing those metallic ions, the resultant sludge is hazardous to the environment and living beings, requiring expensive treatment or landfill disposal [7–9].

Electrochemical treatment methods are attractive since they can combine metal removal with metal recovery in its pure form, without sludge generation [10, 11]. As an example, electrolysis can be used to recover metals from industrial effluents. However, most electrolytic processes are ineffective at low metal concentrations since their effectiveness is dependent on the mass-transfer rate of the metal ions from the solution to the cathode surface [12]. At low metal concentrations the process becomes difficult and parasitic reactions take place, decreasing the current and removal efficiencies.

Three-dimensional porous electrodes have been frequently used for the removal of toxic metals from real and simulated wastewaters [13–17]. Their large-active surface area allows operation at a low current density [18] and the improvement of the mass-transfer coefficients when combined with the electrolyte recirculation [19]. These features have led to the investigation of different cathode materials and cell designs [8, 20–23]. As reported by Zadra et al. [24], steel wool was one of the first materials employed as three-dimensional porous electrodes. This metallic material was used for recovering gold and silver from activated carbon by leaching and electrolysis. The removal of copper, zinc and lead was investigated by Bertazzoli et al. [2], using reticulated vitreous carbon (RVC) as cathode. By varying the flow rate and the RVC porosity, they were able to reduce the ion concentrations from 50 ppm to 0.1 ppm. Ragnini et al. [8] performed experiments on Pb(II) removal with a three-dimensional niobium-felt cathode. The lead concentration was decreased from 50 ppm to 0.5 ppm for

---

L. C. Almeida · L. H. S. Gasparotto · N. Bocchi (✉) ·
R. C. Rocha-Filho · S. R. Biaggio
Departamento de Química, Universidade Federal de São Carlos,
Caixa Postal 676, Sao Carlos, SP 13560-970, Brazil
e-mail: bocchi@dq.ufscar.br

electrolysis times ranging from 94 min to 150 min, depending on the flow rate. In previous work [23], we reported on the potential of a stainless-steel wool (SSW) cathode, a cheaper material when compared to RVC, to remove Pb(II) from simulated wastewaters. At –0.90 V vs. SCE and flow rate of 250 L h^{-1}, after a 90-min electrolysis the Pb(II) concentration was reduced from 50 ppm to 1 ppm.

In all these studies, experiments were carried out by changing one of the variables and fixing the others. However, the variables may interact strongly. These interactions can be determined using a factorial design of a limited set of variables, which also allows determination of the optimal conditions, due to its capacity for extracting relevant information from the system under study [25]. Another advantage of the factorial design is the possibility to find the smallest number of experiments that must be carried out to obtain the desired information with statistically acceptable results.

In this work the removal of Pb(II) from a simulated wastewater was investigated under galvanostatic condition using the same flow-through cell with a SSW as previously employed [23]. Moreover, independent variables such as the current and the flow rate were simultaneously studied through a factorial design and analysed by the response surface methodology (RSM) [26, 27] in order to obtain the best experimental condition for removing Pb(II).

2 Experimental

2.1 Reagents and solutions

All chemicals used in this work were of analytical grade and the solutions were prepared using water previously distilled and then deionised with a Milli-Q® system (Millipore). Lead nitrate (Aldrich), sodium nitrate (Merck) and boric acid (Merck) were used to prepare the simulated wastewater (catholyte): 50 ppm $Pb(NO_3)_2$ in 0.10 mol L^{-1} $NaNO_3$ and 0.10 mol L^{-1} H_3BO_3 (pH 4.8) as supporting electrolyte; this electrolyte was also used as the anolyte. Atomic absorption standard solutions used in the analyses were prepared using a Titrisol standard solution from Merck.

2.2 Instrumentation

The electrochemical experiments were carried out using an Eco Chemie Autolab/PGSTAT30 galvanostat/potentiostat controlled by the GPES software. An Olympus BX 41 microscope was used to image fibres of the SSW in order to estimate their specific surface area. The catholyte was sampled at predetermined times and its Pb(II) concentration analysed by a Varian SpectrAA 200 spectrophotometer using an air/acetylene flame.

2.3 Experimental design

The efficiency of a galvanostatic electrolytic process is directly influenced by factors such as the current, the electrolyte flow rate and the specific surface area of the electrode. Therefore, these parameters were studied through factorial designs to estimate their influence on the process and also to optimise the Pb(II) removal. Firstly, two Amway® SSWs with different masses (~8 g and ~18 g) and, consequently, distinct specific surface areas were subjected to 2^2-factorial designs with the current and the flow rate as independent variables. The evaluation of the preliminary results suggested that the SSW with the highest mass should be used in further experiments. Then, this SSW was subjected to a central composite rotatable design (CCRD) [28] with two independent variables and three replicates in the central point, totaling 11 experiments (Table 1). Five levels of each independent variable were

Table 1 Coded levels and real values for the central composite rotatable design (CCRD)

Run	Coded levels		Real values		Responses	
	X_1	X_2	X_1	X_2	*CE* (%)	*RE* (%)
1	–1	–1	–0.17	180	8.60	27.30
2	–1	+1	–0.17	320	8.51	30.42
3	+1	–1	–0.31	180	14.12	91.95
4	+1	+1	–0.31	320	15.05	89.83
5	–1.41	0	–0.14	250	8.07	24.33
6	+1.41	0	–0.34	250	13.70	93.19
7	0	–1.41	–0.24	150	16.19	81.24
8	0	+1.41	–0.24	350	19.23	86.08
9	0	0	–0.24	250	21.77	93.53
10	0	0	–0.24	250	21.83	93.79
11	0	0	–0.24	250	20.54	91.84

X_1 = current (A); X_2 = flow rate (L h^{-1})

chosen and the results were analysed by a least-squares method. The data were fitted as second order equations with the software STATISTICA® 6.0 in order to generate the response surfaces [26, 27].

2.4 Procedure for Pb(II) removal

Figure 1 shows a scheme of the electrochemical cell used for lead removal. The cell was made from five PVC circular plates mounted in a “sandwich-like” shape and divided into one cathodic and two anodic compartments, separated by two Nafion® 324 membranes (Du Pont). An Amway® SSW (~18 g) was fixed inside the cathodic compartment by pressing it against a stainless-steel ring. A picture of this SSW is shown in Fig. 2a. Two copper wires were welded to the stainless-steel ring to provide electrical contact. The dual continuous-flow cell design is fully described elsewhere [23]. The assembled system was loaded with 2 L of catholyte. The anolyte was placed in a separate reservoir. The performance of the cell was simultaneously evaluated using the CCRD, mentioned above in Sect. 2.3. The catholyte was periodically sampled and analysed by atomic absorption spectrophotometry.

3 Results and discussion

3.1 The SSW specific surface area

Figure 2b presents a typical micrograph of a single SSW fibre used as cathode in the electrochemical cell. From images obtained for 10 fibre samples, their dimensions (width, thickness and length per mass unit) were measured with the aid of a microscope software (see Fig. 2b). Then the physical parameters of the whole SSW were estimated by relating its mass with the fibre’s superficial area per mass unit. The values obtained for the average dimensions of the SSW fibres, their respective standard deviations and also the SSW specific surface area (A_e) determined by using Eq. 1 [29] are shown in Table 2.

$$A_e = (1-\theta)\frac{S_f}{V_e} \tag{1}$$

where S_f is the SSW surface area, V_e the SSW volume and θ the average void fraction, which is obtained using the relationship $\theta = (V - V_e)/V$, with $V = 63.6 \times 10^{-6}\ \mathrm{m}^3$, the volume of the SSW compartment in the electrochemical cell.

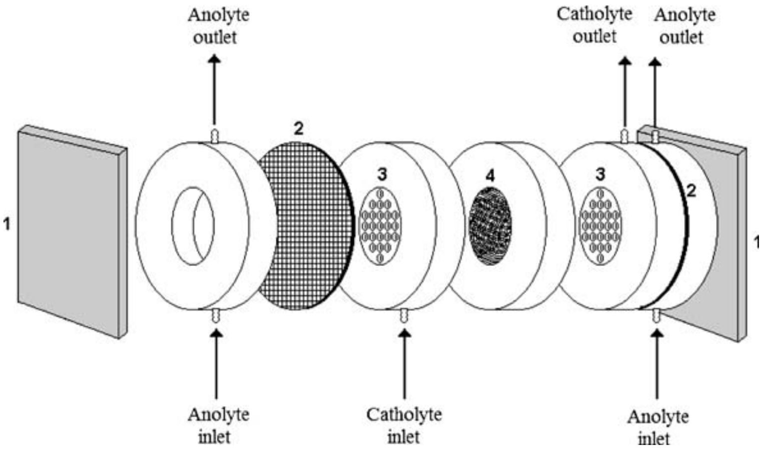

Fig. 1 Expanded view of the cell with a stainless-steel wool cathode: (1) stainless steel anodes, (2) cationic membranes, (3) turbulence promoters and (4) stainless-steel wool cathode

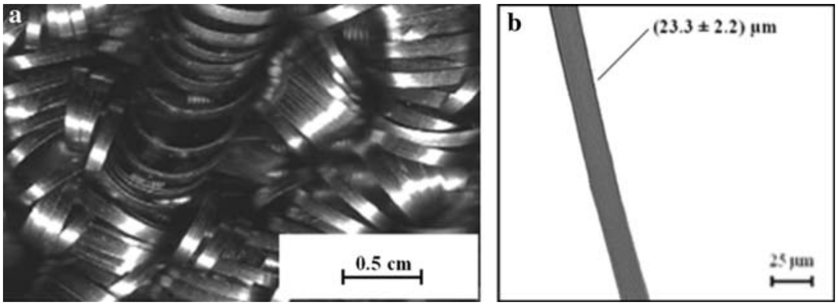

Fig. 2 (**a**) Picture showing a view of the SSW and (**b**) typical micrograph of a single fibre used to estimate the SSW specific surface area

Table 2 Average dimensions of the SSW fibres and physical properties of the whole SSW used as cathode (m = 18.004 g)

Width	$(442.0 \pm 12.9) \times 10^{-6}$ m
Thickness	$(23.3 \pm 2.2) \times 10^{-6}$ m
Length per unit mass	9.54 ± 0.33 m/g
SSW surface area (S_f)	$(1.60 \pm 0.08) \times 10^{-1}$ m^2
SSW volume (V_e)	$(1.77 \pm 0.10) \times 10^{-6}$ m^3
Average void fraction (θ^a)	0.97 ± 0.06
Specific surface area (A_e)	$(2.71 \pm 0.33) \times 10^3$ m^2/m^3

[a] $\theta = (V - V_e)/V$, with $V = 63.6 \times 10^{-6}$ m^3, the volume of the SSW compartment in the cell

3.2 Optimization of Pb(II) removal

As previously mentioned, preliminary electrowinning experiments were carried out using two SSW with different masses and, consequently, distinct specific surface areas. With the SSW of lowest surface area only 50% of Pb(II) removal was achieved after a 30-min electrolysis (data not shown), even for the highest flow rate and current. On the other hand, with the SSW of highest surface area more than 90% of Pb(II) removal was obtained in the same time. Therefore, a set of experiments using the CCRD previously cited (Table 1) was conducted only with the SSW of highest surface area.

On the basis of the least-squares method [25], two second-order models describing the removal and current efficiencies were established as a function of two independent variables (current and flow rate). Equations 2 and 3, containing only the statistically significant terms, were obtained at 95% confidence level:

$$RE = 92.19 + 27.73X_1 - 19.64X_1^2 - 7.11X_2^2 \tag{2}$$

$$CE = 21.39 + 2.51X_1 - 5.96X_1^2 - 2.53X_2^2 \tag{3}$$

where RE and CE are the removal and current efficiencies and X_1 and X_2 the current and flow rate, respectively.

Figure 3 presents the response surfaces generated by Eqs. 2 and 3. Although the rate of electrochemical reactions under mass transport conditions is dependent on the flow rate, both responses (removal and current efficiencies) were not substantially affected by this variable. Flow rates in the range of 180–250 L h^{-1} did not lead to significant changes in the mass transfer coefficient [30], while in the range of 250–320 L h^{-1} the generation of dead zones in the cell and/or electrolyte channeling possibly contributed to decreased reactor performance [31]. On the other hand, increase in current positively influenced the rate of Pb(II) reduction, leading to 93% of removal after 30-min electrolysis. It should be noted that the current efficiency was strongly affected by parasitic reactions. Oxygen reduction is the main electrochemical process occurring in the cathodic current range investigated, leading to lower current efficiencies. Dutra et al. [32] and Gasparotto et al. [23] found that the oxygen reduction process plays the major role in consuming the charge. The maximum current efficiency occurs at –0.25 A, where the conversion of Pb(II) to Pb is the highest. Analysing the surface toward more negative values of current, the current efficiency starts to decrease due to simultaneous O_2, water, and nitrate reduction. However, for less negative current values, the current efficiency also decreases when it should have increased as the values of potential are more negative (Fig. 4) than the potential range (–0.75 to –0.95 V vs. ECS) where the Pb(II) electroreduction is diffusion controlled, as previously showed by Gasparotto et al. [23]. This occurs because the reaction may be under mixed control due to potential distribution for values of current less negative than –0.25 A. It is well known that there is a potential distribution within these porous electrodes [18]. Also, studies carried out by Lanza et al. [7] on Zn(II) removal using RVC as cathode showed that the current penetration depends on the electrode thickness, reinforcing the predictions made by Doherty et al. [18]. Although the

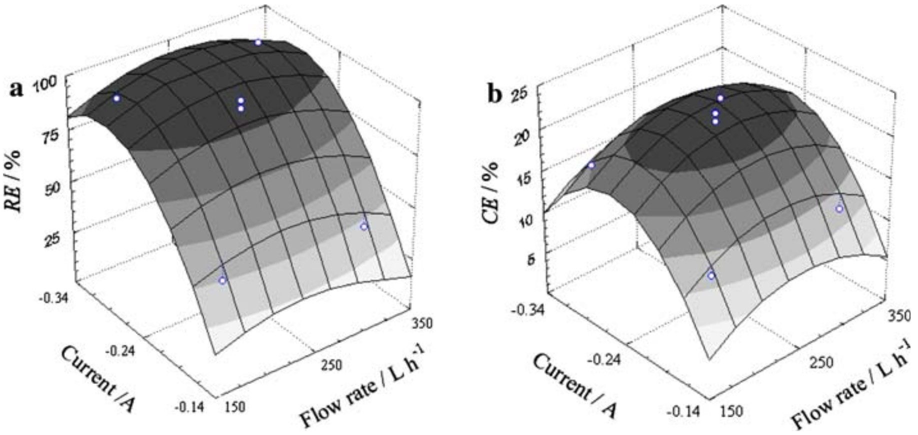

Fig. 3 Response surfaces generate using equations (2) and (3), for (**a**) removal efficiency and (**b**) current efficiency after 30-min electrolysis

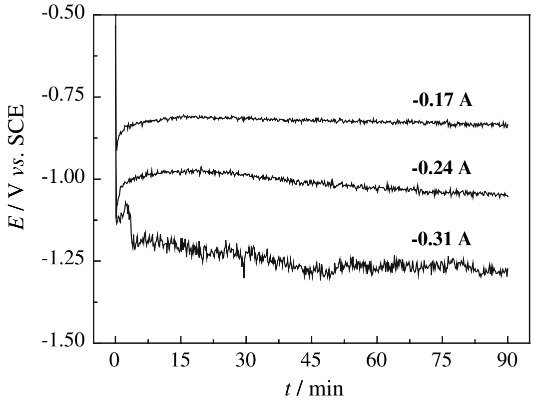

Fig. 4 Chronopotentiograms for Pb(II) removal on the SSW electrode at 250 L h^{-1} and different currents

current efficiencies were relatively low, they are higher than those reported in the literature [19, 23, 33].

The analysis of variance (ANOVA) was used to numerically evaluate the adequacy of both square-fitted models (removal and current efficiencies). By the analysis of variance presented in Tables 3 and 4, and based on the *F*-test, it was found that the models predict well the cell behaviour operating in the current and flow rate ranges investigated, as the calculated *F*-ratios were higher than the critical one (5.05 at 95% confidence level) and the regression coefficients were close to unity. The plots of the residual versus fitted values (Fig. 5) did not indicate any problems with the models since the residuals were randomly distributed, confirming the appropriateness of the models used. Probability plots were also obtained (Fig. 6) for evaluating the significance of the terms for both models (removal and current efficiencies). All terms different from zero were considered statistically significant.

The RSM was a valuable tool for locating the optimal conditions to be applied to the electrochemical cell. The surfaces formed revealed that the region around –0.25 A and 250 L h^{-1} was the best for Pb(II) removal. Figure 7 depicts the normalized Pb(II) concentration depletion as a function of electrolysis time obtained at –0.25 A and 250 L h^{-1}. The Pb(II) concentration exponential decay indicates a mass-transfer-controlled reaction [34]. This was confirmed by the linear ln [C/C_0] versus time plot shown in the inset, whose slope gives an indication of the cell performance as it is related to the mass transfer coefficient (k_m) [35]. A Pb(II) removal of 94% was achieved after 30 min when the electrolysis was carried out at the optimal

Table 3 Summary of the ANOVA with the data obtained using the CCRD (Table 1) for the removal efficiency (*RE*) after 30-min electrolysis

Source of variation	Sum of square (SS)	Degrees of freedom (DF)	Mean square (SS)	*F*-ratio (model significance)
Regression (R)	8317.8	5	1663.6	$MS_R/MS_r = 23.45$
Residual (r)	354.64	5	70.928	
Lack of Fit (Lf)	340.87	3	113.62	
Pure error (Pe)	13.775	2	6.8874	
Total	8672.4	10	–	

Regression coefficient (SS_R/SS_T): 0.960; $F_{5,5}$ (at 95% confidence level) = 5.05

Table 4 Summary of the ANOVA with the data obtained using the CCRD (Table 1) for the current efficiency (*CE*) after 30-min electrolysis

Source of variation	Sum of square (SS)	Degrees of freedom (DF)	Mean square (MS)	*F*-ratio (model significance)
Regression (R)	256.47	5	51.294	$MS_R/MS_r = 13.52$
Residual (r)	18.964	5	3.7929	
Lack of fit (Lf)	17.904	3	5.9681	
Pure error (Pe)	1.0602	2	0.5301	
Total	275.44	10	–	

Regression coefficient (SS_R/SS_T): 0.931; $F_{5,5}$ (at 95% confidence level) = 5.05

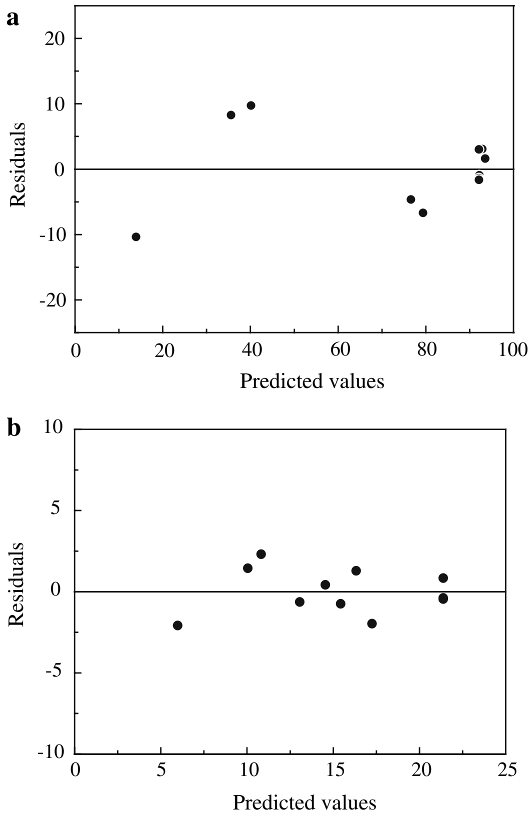

Fig. 5 Residual plots for (**a**) removal and (**b**) current efficiencies models

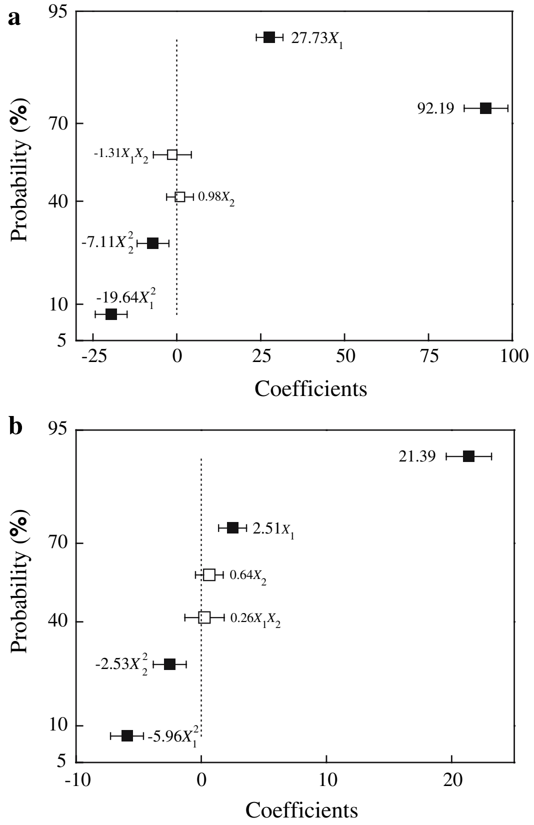

Fig. 6 Normal probability plots of coefficients obtained for (**a**) removal and (**b**) current efficiencies models

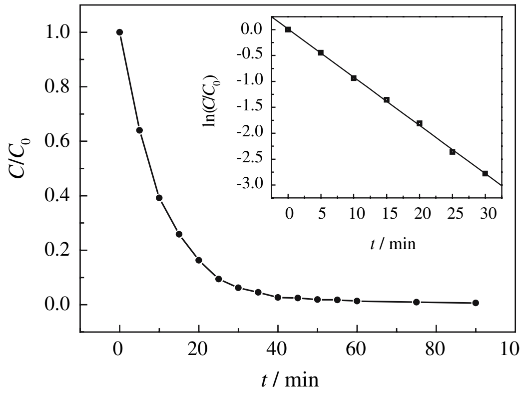

Fig. 7 Normalized concentration (C/C_0) versus time behaviour in the flow-through cell for Pb(II) removal at –0.25 A and 250 L h^{-1}. Inset: Logarithm of the dimensionless lead concentration versus electrolysis time

Table 5 Comparison of results for Pb(II) removal from the simulated wastewater using a stainless-steel wool cathode in a flow-through cell operating in galvanostatic and potentiostatic mode after 30 min-electrolysis

Method	*CE* (%)	*RE* (%)	$k_m \times 10^{-5}$ (m/s)	$t_{90\%}$ (min)
Galvanostatic	22	93	1.8	25
Potentiostatic[a] [23]	17	81	1.3	42

[a] at –0.90 V vs. SCE and 250 L h^{-1}

point (–0.25 A and 250 L h^{-1}). Furthermore, after 90-min electrolysis a concentration of only 0.5 ppm was reached, corresponding to 99% of removal. Comparing these results (Table 5) with those previously obtained by Gasparotto et al. [23], it is evident that the surface response methodology helped to obtain an improved electrochemical system performance. Two changes in the electrochemical cell (improvement of the turbulence promoters and a new way to fix the SSW inside the cathodic compartment) also contributed to improve its performance, specially the increase in mass-transfer coefficient. It is important to point out that different values of current and flow rate near the optimal point can also provide similar results, since the RSM gives a region of best performance.

4 Conclusions

The present study provides a practical, efficient, rapid and inexpensive way of treating wastewater containing Pb(II) ions. Factorial design (CCRD) experiments and analyses using the RSM allowed the location of the optimal condition for Pb(II) removal from a simulated wastewater using a SSW cathode in a flow-through cell. According to the experimental and statistical analyses, increasing currents improved the electrochemical cell performance while the flow rate did not substantially affect it. The ANOVA showed that the least-squares fitted models can perfectly predict the performance of the electrochemical cell in the flow rate and current ranges studied. The surfaces formed with the results of the electrowinning experiments revealed that the region around –0.25 A and 250 L h^{-1} was the best for Pb(II) removal. In these conditions, the Pb(II) concentration was diminished from 50 ppm to 0.5 ppm in 90 min, corresponding to 99% removal.

Acknowledgments The authors gratefully acknowledge the Brazilian research funding agencies CAPES, CNPq and FAPESP for financial support and scholarships. The authors also thank Prof. Edenir R. Pereira Filho (Departamento de Química, UFSCar) for discussions on factorial design.

References

1. Ahluwalia SS, Goyal D (2007) Bioresour Technol 98(12):2243
2. Bertazzoli R, Widner RC, Lanza MRV, Di Iglia RA, Sousa MFB (1997) J Braz Chem Soc 8(5):487
3. Walsh FC (2001) Pure Appl Chem 73(12):1819
4. Issabayeva G, Aroua MK, Sulaiman NM (2006) Desalination 194(1–3):192
5. Grau JM, Bisang JM (2005) J Appl Electrochem 35:285
6. Koene L, Janssen LJJ (2001) Electrochim Acta 47(5):695

7. Lanza MRV, Bertazzoli R (1999) J Appl Electrochem 30(1):61
8. Ragnini CAR, Di Iglia RA, Bizzo W, Bertazzoli R (2000) Water Res 34(13):3269
9. Reyes-Cruz V, Gonzalez I, Oropeza MT (2004) Electrochim Acta 49(25):4417
10. Elsherief AE (2003) Electrochim Acta 48(18):2667
11. Kaminari NMS, Schultz DR, Ponte M, Ponte HA, Marino CEB, Neto AC (2007) Chem Eng J 126(2–3):139
12. Jüttner K, Galla U, Schmieder H (2000) Electrochim Acta 45:2575
13. Langlois S, Coeuret F (1989) J Appl Electrochem 19(1):51
14. Ruotolo LAM, Gubulin JC (2002) Braz J Chem Eng 19(1):105
15. Simonsson D (1984) J Appl Electrochem 14(5):595
16. Sioda RE, Piotrowska H (1980) Electrochim Acta 25(3):331
17. Lemos FA, Sobral LGS, Dutra AJB (2006) Miner Eng 19(5):388
18. Doherty T, Sunderland JG, Roberts EPL, Pickett DJ (1996) Electrochim Acta 41(4):519
19. Widner RC, Sousa MFB, Bertazzoli R (1998) J Appl Electrochem 28(2):201
20. Cachet C, Wiart R, Zoppasferreira J (1993) Electrochim Acta 38(2–3):311
21. Matlosz M, Newman J (1986) J Electrochem Soc 133(9):1850
22. Oren Y, Soffer A (1983) Electrochim Acta 28(11):1649
23. Gasparotto LHS, Bocchi N, Rocha RC, Biaggio SR (2006) J Appl Electrochem 36(6):677
24. Zadra JB, Engel AL, Heinen HJ (1952) US Bureau of Mines Report of Investigations 4843
25. Bruns RE, Scarminio IS, Neto BB (2006) Statistical design-chemometrics. Elsevier, Amsterdam
26. Box GEP, Draper NR (1987) Empirical model-building and response surfaces. Wiley, New York
27. Myers RH, Montgomery DC (2002) Response surface methodology. Wiley, New York
28. Box GEP, Hunter WG, Hunter JS (1978) Statistics for experimenters. Wiley, New York
29. Coulson JM, Richardson JF (1968) Chemical engineering. Pergamon Press, London
30. Ruotolo LAM, Gubulin JC (2005) Chem Eng J 110(1–3):113
31. Levenspiel O (1972) Chemical reaction engineering. Wiley, New York
32. Dutra AJB, Espinola A, Borges PP (2000) Miner Eng 13 (10–11):1139
33. Leon CPD, Pletcher D (1996) Electrochim Acta 41(4):533
34. Pletcher D, Whyte I, Walsh FC, Millington JP (1991) J Appl Electrochem 21(8):667
35. Walker ATS, Wragg AA (1977) Electrochim Acta 22(10):1129